Independent and Cooperative Roles of *N*-Glycans and Molecular Chaperones in the Folding and Disulfide Bond Formation of the Low-Density Lipoprotein (LDL) Receptor-Related Protein†

Lynn M. McCormick,‡ Reiko Urade,§ Yukino Arakaki,§ Alan L. Schwartz,‡ and Guojun Bu*,‡

Department of Pediatrics and Department of Cell Biology and Physiology, Washington University School of Medicine, St. Louis, Missouri 63110, and Graduate School of Agriculture, Kyoto University, Uji, Kyoto 611-0011, Japan

Received November 4, 2004; Revised Manuscript Received February 3, 2005

ABSTRACT: The low-density lipoprotein receptor-related protein (LRP) is a large receptor that contains extensive glycosylation sites and disulfide bonds. Here we analyzed how N-linked glycosylation and molecular chaperones function during LRP folding. Treatment of cells with a glycosylation inhibitor tunicamycin significantly impaired LRP folding, although binding to receptor-associated protein (RAP), a specialized chaperone for LRP, was not affected. The effects of tunicamycin on LRP folding were not due to an inhibition of RAP glycosylation since a mutant RAP that harbors a mutation at its sole glycosylation site was still capable of promoting LRP folding. The roles of N-linked glycosylation and the lectin chaperone, calnexin, in LRP folding were further dissected using LRP minireceptors that carry mutations at individual glycosylation sites. Interestingly, we found that RAP interacts with oxidoreductase ERp57 and mediates its interaction with LRP. Since previous studies have shown that *N*-glycan-bound calnexin/calreticulin are also capable of recruiting ERp57, our results suggest that N-linked glycosylation and RAP can independently and cooperatively recruit oxidoreductases to facilitate protein folding and proper disulfide bond formation.

The low-density lipoprotein (LDL)[1] receptor-related protein (LRP) is a member of the LDL receptor family and one of the largest cell surface receptors identified to date (~600 kDa) (*1*, *2*). LRP is capable of binding and endocytosing a large array of ligands, many of which are structurally and functionally distinct. Biochemical studies have shown that LRP is synthesized as a single polypeptide chain that is cleaved by furin in the trans-Golgi network into two subunits of 515 kDa and 85 kDa, which remain associated with one another as they mature to the cell surface (*3*, *4*). The 515 kDa amino-terminal subunit contains 31 ligand-binding repeats grouped into four clusters of 2, 8, 10, and 11 repeats and separated by epidermal growth factor (EGF)-like repeats and β-propeller-like structures that contain the YWTD motifs (*5*), whereas the 85 kDa subunit includes a single transmembrane domain and a 100-amino acid cytoplasmic tail. The three-dimensional structures of several ligand-binding repeats have been solved via either protein crystallization or NMR analysis (*6*−*9*). These studies show that, in addition to the three disulfide bridges, each ligand-binding repeat coordinates a Ca^{2+} ion, which forms an octagonal structure with neighboring acidic amino acid residues and plays an essential role in LRP folding (*10*, *11*).

The complex structures of LRP, largely due to the extensive intradomain disulfide bonds (159 disulfide bonds within its ligand-binding and EGF repeats), present a challenging task to their proper folding during biosynthesis within the endoplasmic reticulum (ER). Cooperative actions of both general ER chaperones (e.g., BiP, protein disulfide isomerase (PDI), and calnexin) and specialized chaperone(s) are likely required to achieve proper folding for such a complex receptor. Indeed, our previous studies have shown that proper folding of both soluble (*12*) and transmembrane domain-containing (*11*, *13*, *14*) LRP minireceptors is facilitated by the coexpression of receptor-associated protein (RAP), a specialized chaperone for members of the LDL receptor family. In the absence of RAP coexpression, LRP minireceptors oligomerize due to formation of mislinked intermolecular disulfide bonds and are retained within the ER. Our studies also showed that the functions of RAP and Ca^{2+} ions during LRP folding are independent with Ca^{2+} ions likely serving as a nucleation site during initial folding of ligand-binding repeats. Unlike most of the ER chaperones, which dissociate from folded substrates, RAP remains associated with LRP following receptor folding and during its subsequent trafficking (*15*). Because RAP universally antagonizes ligand binding to LRP, it is hypothesized that the physiological significance of RAP association with LRP is to prevent premature ligand interaction with the receptor during its trafficking through the secretory pathway (*16*, *17*).

† This work was supported by National Institutes of Health Grant DK61761 (to G.B.). G.B. is an Established Investigator of the American Heart Association.

‡ Washington University School of Medicine.

§ Kyoto University.

* To whom correspondence should be addressed. Department of Pediatrics, Washington University School of Medicine, CB 8208, 660 South Euclid Avenue, St. Louis, MO 63110; phone, (314)286-2860; fax, (314)286-2894; e-mail, bu@wustl.edu.

[1] Abbreviations: LDL, low-density lipoprotein; LRP, LDL receptor-related protein; EGF, epidermal growth factor; RAP, receptor-associated protein; PDI, protein disulfide isomerase; ER, endoplasmic reticulum; MEF, mouse embryonic fibroblasts; SPR, surface plasmon resonance.

10.1021/bi047652a CCC: $30.25
Published on Web 03/17/2005

The dual functions of RAP in LRP folding and trafficking suggest that RAP is a unique specialized chaperone and likely coordinates with general ER chaperones in the complex folding process of LRP. Recent studies have identified another specialized chaperone for members of the LDL receptor family, termed Mesd (mesoderm development) in mouse (*18*) and Boca in *Drosophila* (*19*). This new chaperone was discovered due to its requirement for the folding of LRP5/LRP6, coreceptors for the Wnt signaling pathway (*20*). It was shown that Mesd/Boca plays an important role in the folding and maturation of the β-propeller/EGF modules in LDL receptor family members. The mechanisms underlying the role of RAP and Mesd in promoting specialized modules present in the LDL receptor family members are not clear at present.

Previous studies have shown that N-linked glycosylation is required for proper folding of newly synthesized influenza hemagglutinin (HA) and vesicular stomatitis virus G protein (*21*, *22*). These modifications are likely involved in the binding of chaperones such as calnexin and calreticulin (*23*). Alternatively, they may be directly involved in folding by providing spatial constraints or an optimal local environment necessary for protein folding (*24*). Since LRP contains a large number of potential N-linked glycosylation sites, we investigated the roles of these modifications in LRP folding and how they are related to those of molecular chaperones. We found that N-linked glycosylation is essential for the proper folding of LRP independent of RAP. We also found that RAP is capable of mediating interactions between general ER chaperones and LRP, suggesting a cooperative role between specialized and general ER chaperones.

EXPERIMENTAL PROCEDURES

Cell Culture. Human hepatoma HepG2 cells were cultured in MEM supplemented with 10% fetal calf serum, 100 units/mL of penicillin, and 100 μg/mL of streptomycin and maintained at 37 °C in humidified air containing 5% CO_2. Mouse embryonic fibroblast (MEF)-7 cells (*25*) and human glioblastoma U87 cells (*26*) were cultured under the same conditions, except DMEM was used in place of MEM.

Metabolic Pulse-Chase Labeling. Metabolic labeling with [^{35}S]cysteine was performed essentially as described before (*15*). Briefly, cells were generally pulse-labeled for 30 min with 200 μCi/mL of [^{35}S]cysteine in cystine-free medium and chased with serum-containing medium for various times as indicated in each experiment. For inhibition of glycosylation, 20 μg/mL of tunicamycin was preincubated with cells for 1 h and was included in the pulse-labeling and chase media. Cells were lysed in ice-cold PBSc (phosphate-buffered saline supplemented with 1 mM $CaCl_2$ and 0.5 mM $MgCl_2$) containing 1% Triton X-100 and protease inhibitor cocktail Complete (Roche). *N*-ethylmaleimide (NEM) at 10 mM was also included in the lysis buffer to protect free −SH groups.

LRP Minireceptors and Site-Directed Mutagenesis. Soluble (*12*) and transmembrane domain-containing (*14*) LRP minireceptors, representing individual ligand-binding domains, were constructed and described previously. All LRP minireceptors contain an HA tag after the signal cleavage site. Site-directed mutagenesis of RAP and mLRP4 were performed using the QuikChange Mutagenesis Kit (Stratagene) according to the manufacturer's instructions. All cDNA constructs from mutagenesis were verified by DNA sequencing.

Transient Transfection. HepG2 cells at 20−30% confluence were transiently transfected with various plasmids using a calcium phosphate precipitation method (*15*). Initial transfection was performed in 10 cm dishes using 40 μg of DNA in a total volume of 15 mL of medium. Sixteen hours after the start of transfection, cells were washed with medium and cultured continuously for an additional 4 h before being split into multiple 6-well dishes (3.5 cm in diameter) for various pulse−chase experiments.

Antibodies, Immunoprecipitation, Western Blotting, and SDS−PAGE. Rabbit polyclonal anti-LRP (generated against purified human LRP) and anti-RAP (generated against recombinant human RAP) antibodies have been described before (*15*). Monoclonal anti-HA antibody was obtained from Roche (clone 12CA5). Anti-calnexin antibody was purchased from Stressgen. Immunoprecipitations were carried out essentially as described before (*27*), except the washing buffer for monoclonal anti-HA antibody contained 0.1% SDS instead of 1% SDS. Native conditions for co-immunoprecipitation was performed in cell lysis buffer without SDS. Preliminary experiments were performed to ensure that the primary antibody used in each immunoprecipitation was in excess. Protein A-agarose beads were used to precipitate protein−IgG complexes. The immunoprecipitated material was released from the beads by boiling each sample for 5 min in Laemmli sample buffer (62.5 mM Tris-HCl, pH 6.8, 2% (w/v) SDS, and 10% (v/v) glycerol) (*28*). If the immunoprecipitated material was analyzed under reducing conditions, 5% (v/v) β-mercaptoethanol was included in the Laemmli sample buffer. For Western blotting, secondary antibodies (goat-anti-mouse IgG or goat anti-rabbit IgG) were detected with ECL Plus (Amersham Biosciences). Rainbow molecular weight markers (Bio-Rad) were used as the molecular weight standards.

Ligand Dot-Blotting. PVDF membranes (Millipore) were prewet in methanol and equilibrated in PBS. Membranes were then mounted in a Bio-Rad dot-blot apparatus. Purified LRP from human placenta (1 μg/well) was applied to the membrane by vacuum filtration. The membrane was then cut into sections that were placed in separate wells of a 24-well plate. Membranes were blocked in Tris-buffered saline (20 mM Tris-HCl, pH 7.4, and 150 mM NaCl) containing 5 mM $CaCl_2$ and 3% nonfat dry milk for 30 min. Test proteins were incubated with each membrane spot for 2 h at room temperature. Individual spots were washed twice for 5 min with blocking buffer and further incubated with anti-RAP or anti-ERp57 antibodies in the same buffer for 1 h at room temperature to detect binding of the ligand to LRP.

Surface Plasmon Resonance (SPR). The sensor chip was activated with a 1:1 mixture of *N*-hydroxysuccinimide/*N*-ethyl-*N*-*N*′-(3-dimethylaminopropyl)carbodiimide hydrochloride. ERp57 was immobilized in a 10mM sodium acetate buffer at pH 4.0, and the remaining binding sites were blocked with 1 M ethanolamine, pH 8.5. A control channel on the sensor chip was activated and blocked using amino-coupling reagents without immobilization of protein. The binding of the protein to this control channel was subtracted from the specific binding. The flow buffer contains various concentrations of RAP or RAP repeat constructs in 10 mM

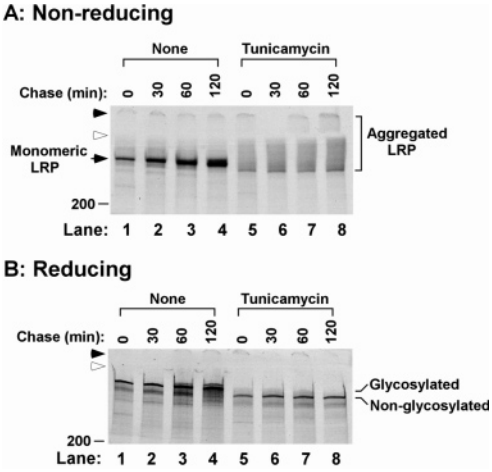

FIGURE 1: N-linked glycosylation is required for LRP folding. HepG2 cells were metabolically pulse-labeled with [^{35}S]cysteine for 30 min and chased for indicated times. The pulse−chase labeling was performed either in the absence or presence of 20 μg/mL tunicamycin. Cell lysates were then immunoprecipitated with anti-LRP antibody and analyzed via 5% SDS−PAGE under either nonreducing (A) or reducing (B) conditions. In this and subsequent figures, the positions of monomeric LRP and aggregated LRP in the nonreducing gels are marked, and the top of the stacking and separating gels are marked with closed and open arrows, respectively. The 200-kDa molecular size markers are also indicated. Note LRP forms intermolecular disulfide-bond-linked aggregates (A, labeled with a bracket) in the presence of tunicamycin, which was reduced to monomers under reducing conditions (B). The glycosylated (without tunicamycin) and nonglycosylated (with tunicamycin) LRP in (B) are labeled.

Hepes, pH 7.4, 0.15 M NaCl, 0.05% Tween 20, and 3 mM $CaCl_2$. In some experiments, 1 mM DTT was included in the flow buffer. The binding data were analyzed by nonlinear least squares curve fitting. Association and dissociation rate constants, k_a and k_d were generated from the association and dissociation curves from the BIAcore experiments by fitting to a single-site or two-sites binding model depending on the results of comparison fitting with these models, respectively. The apparent equilibrium dissociation constant K_D was determined from the ratio of two rate constants (k_d/k_a).

RESULTS

N-Linked Glycosylation Is Required for LRP Folding. The large number of potential N-linked glycosylation sites in LRP prompted us to examine their role in LRP folding. To block LRP glycosylation in cultured cells, we utilized tunicamycin, a nucleoside antibiotic that inhibits N-linked glycosylation. HepG2 cells, which express abundant LRP (*27*), were metabolically pulse-labeled with [^{35}S]cysteine for 30 min and chased for up to 2 h (Figure 1). The pulse−chase labeling was performed either in the absence or presence of 20 μg/mL of tunicamycin. Cell lysates were then immunoprecipitated with anti-LRP antibody and analyzed via SDS−PAGE under either nonreducing (Figure 1A) or reducing (Figure 1B) conditions. As seen in Figure 1A, LRP forms intermolecular disulfide-bond-linked aggregates in the presence, but not in the absence, of tunicamycin, suggesting that LRP is misfolded (*11*) when glycosylation of the nascent receptor was inhibited. The effectiveness of tunicamycin treatment was evident from faster migrating bands when LRP immunoprecipitates were analyzed under reducing conditions (Figure 1B). These results clearly indicate that N-linked glycosylation is required for the proper folding of LRP.

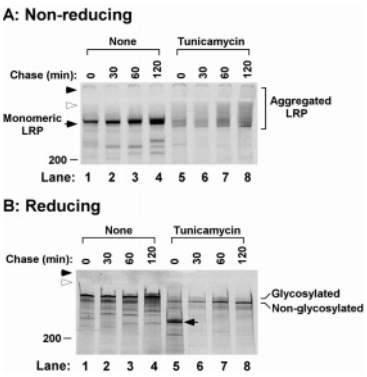

FIGURE 2: RAP binds to nonglycosylated LRP during folding. HepG2 cells were metabolically pulse−chase-labeled as in Figure 1. Cell lysates were then co-immunoprecipitated with anti-RAP antibody under native conditions (no SDS) and analyzed via 5% SDS−PAGE under either nonreducing (A) or reducing (B) conditions. Note anti-RAP antibody co-immunoprecipitated LRP both in the absence and presence of tunicamycin treatment, including those of intermolecular disulfide-bond-linked aggregates (labeled with a bracket). The arrow in B (lane 5) represents either incompletely translated or partially degraded LRP species.

Previous studies have shown that binding of RAP to LRP is partially inhibited by wheat germ agglutinin (WGA) lectin (*29*), suggesting a potential role of LRP glycosylation in RAP binding. Therefore, one possible consequence of blocking LRP glycosylation is inhibition of RAP association with the receptor during folding (*16*). Since RAP itself plays an important role in LRP folding (*16*), a disruption of RAP binding may have an indirect consequence on LRP folding. To address this possibility, we performed identical pulse−chase labeling of LRP in HepG2 cells as described above in Figure 1 in the absence or presence of tunicamycin, except that the resulting cell lysates were immunoprecipitated with either an anti-RAP antibody or preimmuno IgG under native conditions which preserve RAP−LRP interaction (*15*). As seen in Figure 2, anti-RAP antibody co-immunoprecipitated LRP both in the absence and presence of tunicamycin treatment. Preimmuno IgG did not immunoprecipitate any radiolabeled proteins in the absence or presence of tunicamycin treatment (data not shown). The fact that aggregated LRP was also co-immunoprecipitated with RAP suggests that LRP misfolding alone does not impair RAP binding. These results are consistent with those from our previous studies (*11*) showing that aggregated LRP upon calcium-depletion also binds to RAP. The association of LRP with RAP in the presence of tunicamycin is highly specific as LRP appears to be the only major [^{35}S]-labeled protein that co-immunoprecipitated with RAP, despite the presence of other misfolded glycoproteins. Together, these results demonstrate that RAP binding to LRP during its initial folding does not require N-linked glycosylation.

To further examine whether RAP is able to interact with aggregated LRP, we analyzed the ability of ^{125}I-RAP to bind native, aggregated or completely reduced LRP. Aggregation of LRP was induced by incubation of purified LRP from human placenta with low concentrations of reducing reagent (DTT) at 37 °C for 1 h. As seen in Figure 3A, after incubation of purified native LRP at 37 °C for 1 h, LRP has become misfolded and migrated as heterogeneous species

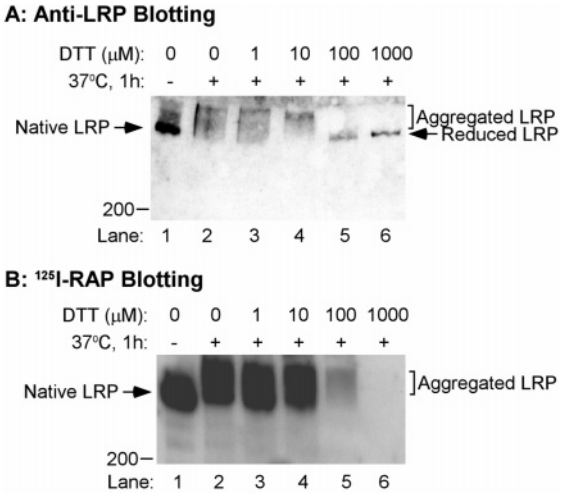

FIGURE 3: RAP binds to native and aggregated LRP. Purified LRP (100 ng/lane) was either used direct (lane 1) or used following incubation at 37 °C for 1 h in the absence (lane *2*) or presence of increasing concentrations of DTT as indicated (lanes 3−6). Following separation by 5% SDS−PAGE under nonreducing conditions, the membrane was either Western-blotted with anti-LRP antibody (A) or ligand-blotted with ^{125}I-RAP (1 nM, B). The DTT concentration is given in μM. Note, native and aggregated LRP, but not reduced LRP, bind to RAP.

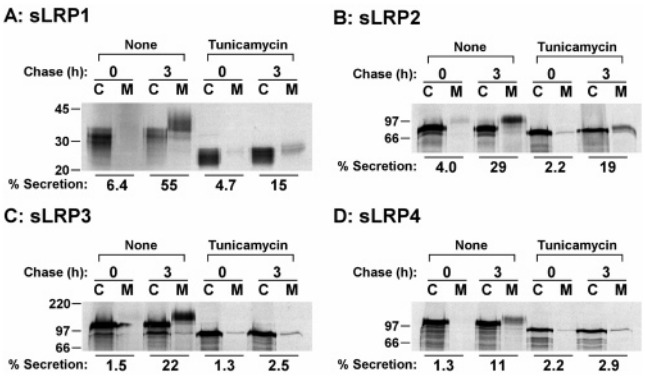

FIGURE 4: Soluble LRP domain minireceptors (sLRPs) are differentially misfolded upon tunicamycin treatment. HepG2 cells were transiently transfected with cDNAs for RAP and sLRP1 (A), sLRP2 (B), sLRP3 (C), or sLRP4 (D). The transfected cells were then metabolically pulse-labeled with [^{35}S]cysteine for 1 h, followed with either no chase or chase for 3 h. The metabolic labeling was carried out in the absence or presence of tunicamycin. Both cell lysates and media were then immunoprecipitated with anti-HA antibody, followed with SDS−PAGE (10% for sLRP1, 7.5% for sLRP2−4) under reducing conditions. The percent of sLRP secretion was quantitated by a phosphorimager and reported under each condition. "C" represents cell lysates, and "M" represents medium. This experiment represents one of several performed with similar results. Note the secreted sLRPs without tunicamycin treatment were larger than those detected in cell lysates due to the addition of complex carbohydrates upon traversing through the Golgi compartments. The reduction in overall sizes for each sLRP upon tunicamycin treatment demonstrates an effective inhibition of their glycosylation.

of intermolecular disulfide-bond-linked aggregates (lane 2). The presence of increasing concentrations of DTT up to 10 μM accelerate the formation of these aggregates (lanes 3 and 4), whereas high concentrations of DTT ($\geq$100 μM) result in complete reduction of LRP (lanes 5 and 6). When the ability of different species of LRP to bind ^{125}I-RAP was analyzed (Figure 3B), we found that, in addition to the native LRP (lane 1), misfolded LRP aggregates retain the ability to bind RAP (lanes 2−4). However, completely reduced LRP lost the ability to bind RAP, suggesting that binding of RAP to LRP requires the presence of certain disulfide bonds.

N-Linked Glycosylation Has Differential Roles in the Folding of LRP Individual Domains. The effects of tunicamycin on LRP folding were also observed with membrane-containing LRP domain minireceptors (*14*) (data not shown, and see below in Figure 5). To quantitatively assess the importance of N-linked glycosylation in the folding of individual LRP domains, we analyzed the folding and secretion of soluble LRP minireceptors (sLRPs) that represent the four clusters of ligand-binding and EGF repeats (*12*). Our previous pulse−chase kinetic studies have shown that folding and secretion of these sLRPs are facilitated by coexpression of RAP (*12*). HepG2 cells were transiently transfected with cDNAs for each of the sLRPs and RAP (1:1 plasmid/DNA ratio). The transfected cells were then metabolically pulse-labeled with [^{35}S]cysteine for 1 h, followed with either no chase or chase for 3 h. The metabolic labeling and chase were carried out in the absence or presence of tunicamycin. Both cell lysates and media were quantitatively immunoprecipitated (in the presence of excess antibody) with anti-HA antibody, followed with SDS−PAGE under reducing conditions. The percent of sLRP secretion under each condition was quantitated by a phosphorimager. As seen in Figure 4, the reduction of sLRP secretion upon tunicamycin treatment and 3 h chase was more significant for sLRP1 (55% to 15%), sLRP3 (22% to 2.5%), and sLRP4 (11% to 2.9%) than for sLRP2 (29% to 19%), suggesting that N-linked glycosylation in LRP is more important for the folding of domains I, III, and IV than domain II. This was somewhat surprising since the density of potential N-linked glycosylation sites in domain II is not less than those of other domains (i.e., domain I, 3 sites/166 aa; domain II, 6 sites/458 aa; domain III, 8 sites/543 aa; and domain IV, 5 sites/570 aa). These results indicate that the importance of N-linked glycosylation in protein folding is not solely determined by the number of glycosylation sites present in individual glycoproteins. Small amounts of sLRPs were secreted in the presence of tunicamycin treatment, which might have resulted from incomplete inhibition of sLRP glycosylation by tunicamycin.

N-Linked Glycosylation of RAP Is Not Required for Its Chaperone Function. One possible caveat of experiments using tunicamycin treatment is that tunicamycin also inhibits glycosylation of RAP, which might be required for its chaperone function. To address this, we mutated RAP's single glycosylation site at asparagine residue 234 to alanine (N234A) by site-directed mutagenesis. The mutated RAP cDNA along with wild-type cDNA was transfected into either RAP-null MEF-7 cells (*25*) or HepG2 cells, followed by Western blotting of cell lysates with anti-RAP antibody (Figure 5). In transfected MEF-7 cells, the RAP(N234A) mutant clearly migrated faster than the wild-type RAP, consistent with elimination of RAP glycosylation. Similarly, in HepG2 cells, the RAP(N234A) mutant migrated faster than the wild-type RAP, which comigrates with endogenous RAP. These results indicate that RAP is glycosylated at N234 and mutation of this site eliminates its glycosylation.

To examine whether the nonglycosylated RAP is still functional, we compared the ability of wild-type RAP and RAP(N234A) to promote the folding of LRP domain IV

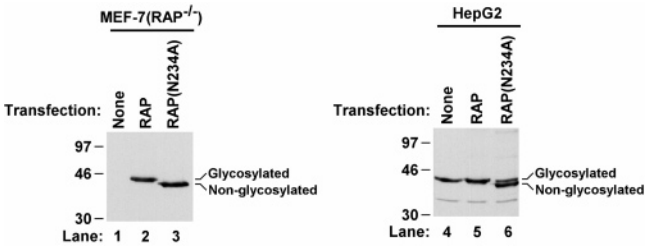

FIGURE 5: RAP is glycosylated at a single site. The asparagine residue 234 of RAP is mutated to alanine by site-directed mutagenesis. RAP-null MEF-7 cells or HepG2 cells were transiently transfected with pcDNA3 vector, pcDNA3−RAP, or pcDNA3−RAP(N234A), followed with SDS−PAGE (10%) and Western blotting of cell lystaes with anti-RAP antibody. The glycosylated RAP in vector-transfected HepG2 cells represents endogenous RAP.

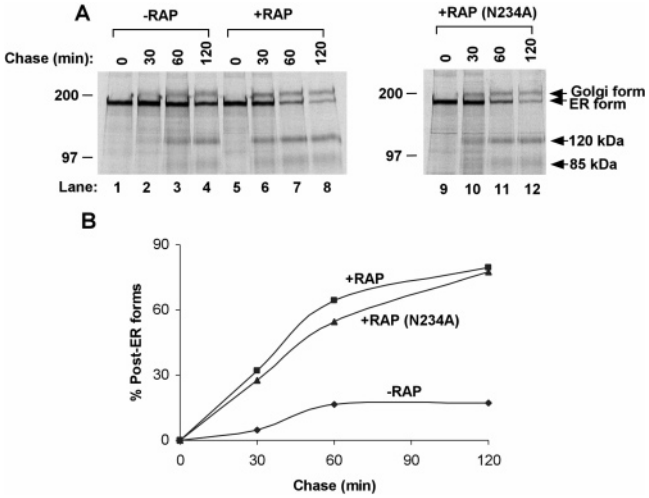

FIGURE 6: N-linked glycosylation of RAP is not required for its chaperone function. HepG2 cells were transiently transfected with cDNA for mLRP4 with cotransfections of pcDNA3 vector (−RAP), wild-type RAP (+RAP), or mutant RAP (+RAP (N234A)). The transfected cells were then metabolically pulse-labeled with [^{35}S]-cysteine for 30 min and chased for indicated times in the absence or presence of tunicamycin. Cell lysates were then immunoprecipitated with anti-HA antibody, followed with SDS−PAGE (7.5%) under reducing conditions (A). The percent of post-ER forms under each condition was quantitated with a phosphorimager and plotted against chase time (B). The results show that both wild-type RAP and nonglycosylated RAP facilitate the folding and trafficking of mLRP4 to similar extent.

minireceptor (mLRP4) (*11*, *14*). Upon proper folding, mLRP4 is processed by furin in the trans-Golgi network to generate a 120 kDa ligand-binding subunit and an 85 kDa transmembrane subunit (*11*, *14*). HepG2 cells were transiently transfected with cDNA for mLRP4 with cotransfections of pcDNA3 vector (−RAP), wild-type RAP (+RAP), or mutant RAP (+RAP(N234A)). The transfected cells were metabolically pulse−chase-labeled as in Figure 1. Cell lysates were then immunoprecipitated with anti-HA antibody, followed with SDS−PAGE under reducing conditions (Figure 6A). The percent of post-ER forms (sum of the Golgi form, 120 kDa, and 85 kDa bands as a percentage of total) under each condition was quantitated with a phosphorimager (Figure 6B). As seen in the figure, both wild-type RAP and nonglycosylated RAP facilitate the folding and trafficking of mLRP4 to similar degrees, suggesting that N-linked glycosylation of RAP is not required for its chaperone function. These results are consistent with the fact that nonglycosylated RAP produced in bacteria is able to bind to cell surface LRP and blocks ligand binding (*16*, *17*).

Individual Glycosylation Sites of LRP Have Differential yet Additive Roles in LRP Folding. Because tunicamycin inhibits N-linked glycosylation of all glycoproteins and also induces unfolded protein response (UPR), we sought for an alternative approach to further address the role of N-linked glycosylation in LRP folding. Therefore, we performed mutagenesis analysis on individual glycosylation sites within mLRP4. This domain IV minireceptor contains only three glycosylation sites within the 11 ligand-binding repeats. Single (N3314A, N3469A, and N3643A), double (N3314A,N3469A; N3469,N3643A; and N3314A,N3643A), or triple (N3314A,N3469A,N3643A) mLRP4 glycosylation mutants were generated by site-directed mutagenesis and analyzed for their abilities to fold properly in the absence or presence of RAP coexpression. Specifically, HepG2 cells were transiently transfected with cDNAs for mLRP4 or its glycosylation mutants without (Figure 7A) or with (Figure 7B) cotransfection of RAP. The transfected cells were metabolically pulse-labeled for 30 min and chased for 120 min, immunoprecipitated with anti-HA antibody, and analyzed via SDS−PAGE under reducing conditions. The percent of post-ER forms under each condition was quantitated with a phosphorimager. A representative autoradiograph of the wild-type mLRP4, as well as a double and the triple mutant, is shown in Figure 7C. As seen in the figure, upon single, double, or triple mutations at individual glycosylation sites on mLRP4, this minireceptor was misfolded to different degrees. The most significant misfoldings were seen with the double mutant mLRP4(N3469A,N3643A) and the triple mutation mLRP4 (N3314A,N3469A,N3643A), suggesting that individual glycosylation sites of LRP likely have additive roles in receptor folding. Interestingly, although individual mutations at N3469 and N3643 residues resulted in little misfolding, simultaneous mutations at both sites gave rise to substantial misfolding (Figure 7A). One possible explanation for these results is that N-linked glycosylation at these two sites has overlapping functions. RAP can partially rescue the misfolding caused by mutations at the glycosylation sites (Figure 7B), including those severely affected by the reduction of *N*-glycans. This suggests that defects in LRP folding due to a reduced number of *N*-glycans do not render the ability of RAP to promote LRP folding.

One role of N-linked glycosylation during protein folding is to interact with molecular chaperones including membrane anchored calnexin (*23*). To analyze the interaction of LRP and LRP minireceptors with calnexin, we performed co-immunoprecipitation analysis. First, we examined interaction between calnexin and the full-length, endogenous LRP. HepG2 cells were lysed and immunoprecipitated with anti-LRP antibody under native conditions. The immunoprecipitated materials were separated via SDS−PAGE, transferred to a membrane, and blotted with the indicated antibodies. As shown in Figure 8A, calnexin can be detected as an LRP-interacting protein. Next, we performed similar co-immunoprecipitation experiments in HepG2 cells transiently transfected with cDNAs of mLRP4 or its glycosylation mutants. Lysates were immunoprecipitated with either anti-HA or anti-calnexin antibodies under native conditions and blotted with anti-HA antibody. We performed these experiments in the absence of RAP coexpression so that a significant portion of these minireceptors would be misfolded

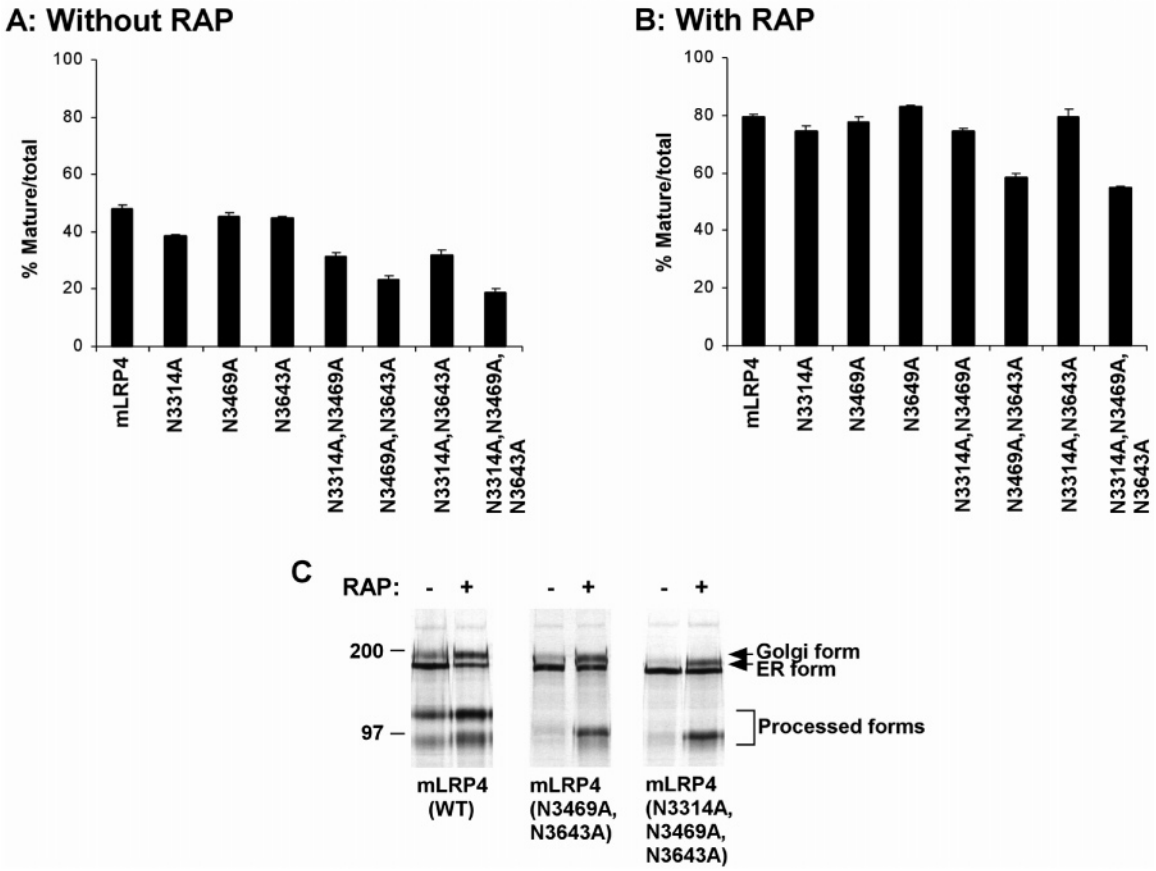

FIGURE 7: Individual glycosylation sites of LRP have differential yet additive roles in LRP folding. HepG2 cells were transiently transfected with cDNA for mLRP4 or one of its glycosylation mutants as indicated, without (A) or with (B) cotransfection of RAP cDNA. The transfected cells were metabolically pulse-labeled with [^{35}S]cysteine for 30 min and chased for 120 min, immunoprecipitated with anti-HA antibody, and analyzed via 7.5% SDS−PAGE under reducing conditions. The percent of post-ER forms under each condition was quantitated with a phosphorimager and plotted for each construct. (C) Representative autoradiograph of wild-type mLRP4 and two glycosylation mutants. Error bars represent SD from triplicate determinations. This experiment represents one of the three such experiments performed with similar results.

(see Figure 7A) and subject to extensive calnexin binding. As shown in Figure 8B, both wild-type mLRP4 and all of its glycosylation mutants were capable of binding calnexin. Importantly, the ability of the glycosylation mutants to interact with calnexin was not diminished by the decrease of glycosylation sites in the mLRP4 minireceptor; that is, double and triple mutants bound to calnexin to a similar extent as the wild-type mLRP4. These results suggest that the ability to interact with calnexin does not necessarily predict the ability of individual glycosylation mutants to fold properly, consistent with the dual roles of calnexin binding in both protein folding (recruiting oxidoreductase) and ER quality control (*23*, *30*). The interaction between calnexin and the mLRP4 triple mutant is likely mediated by the N-linked glycosylation at the potential sites within the EGF repeats and the β-propeller region of the mLRP4 minireceptor. The smear signals on top of the gel following anti-calnexin immunoprecipitation and anti-HA blotting for the glycosylation mutants (e.g., Figure 8B, lower panel, lane 8) likely represent ubiquitinated receptors following their misfolding, although significant degradation of misfolded receptors by the proteasome was not detected (data not shown).

RAP Interacts with ERp57. Our previous studies, and those presented here, demonstrate that RAP promotes LRP folding independent of the roles of Ca^{2+} and N-linked glycosylation. To gain insight into RAP's role in LRP folding, especially in the formation of properly linked disulfide bonds, we explored a cooperative role for RAP with general ER chaperones. Such a cooperative function among ER chaperones is exemplified by calnexin/calreticulin interaction with ERp57 (*31*, *32*). Potential interaction between RAP and several general ER chaperones was first examined via surface plasmon resonance (SPR) analysis. Recombinant ERp57, or several other ER chaperones, was immobilized on the BIAcore sensor chip, and the remaining binding sites on the chip were blocked with ethanolamine. Binding of RAP at various concentrations in the flow buffer to this experimental chip and a control chip was carried out as described in the Experimental Procedures. As shown in Table 1, high affinity binding of RAP to ERp57 was detected. We also found that addition of 1 mM DTT, which would disrupt the disulfide bonds between cysteine residues in the active site CGHC motifs of ERp57 (*33*), reduced interaction between RAP and ERp57 by more than 10-fold (data not shown), suggesting that the oxidation of the active site of ERp57 may be important for RAP binding. Using similar assays, we also detected interactions between RAP and ERp72, PDI, calnexin, and BiP, albeit at lower affinities. Interaction was not detected with calreticulin.

Since ERp57 exhibited the highest affinity to RAP among the ER chaperones tested (Table 1), we further dissected the molecular mechanism underlying the RAP−ERp57 interac-

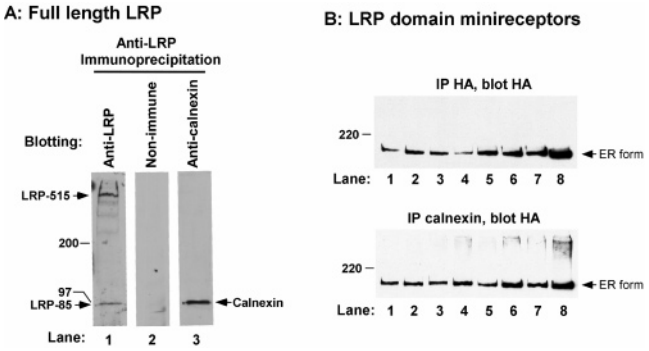

FIGURE 8: Ability to interact with calnexin does not predict the ability of individual glycosylation mutants to fold properly. (A) Lysates from HepG2 cells were immunoprecipitated with anti-LRP antibodies under native conditions (no SDS), followed with immunoblotting with anti-LRP, nonimmune, or anti-calnexin antibodies. LRP-515 kDa and LRP-85 kDa (lane 1), as well as calnexin (lane 3) bands are labeled. (B) HepG2 cells were transiently transfected with cDNAs of mLRP4 or one of its glycosylation mutants, lysed, immunoprecipitated with anti-HA or anti-calnexin antibodies, and blotted with anti-HA antibody. Nonimmune IgG did not immunoprecipitate HA-tagged minireceptors (data not shown). Lane 1, mLRP4; lanes 2−8 are mLRP4 bearing the following mutations at various glycosylation sites: N3314A; N3469A; N3643A; N3314A,N3469A; N3469A,N3643A; N3314A,N3643A; and N3314A,N3469A,N3643A.

Table 1: SPR Analysis of RAP Binding to ER Chaperones[a]

ER chaperones	k_a (1/Ms)	k_d (1/s)	K_A (1/M)	K_D (M)
ERp57[b]	2.71×10^5	5.34×10^{-3}	5.08×10^7	1.97×10^{-8}
ERp72[b]	9.78×10^4	3.47×10^{-2}	2.82×10^6	3.55×10^{-7}
PDI[b]	3.93×10^4	5.75×10^{-3}	6.83×10^6	1.46×10^{-7}
calnexin	1.14×10^4	4.42×10^{-3}	2.58×10^6	3.87×10^{-7}
BiP	2.45×10^4	2.98×10^{-3}	8.22×10^6	1.22×10^{-7}
calreticulin	nd[c]	nd[c]	nd[c]	nd[c]

[a] ER chaperones were immobilized on a sensor chip, and the binding of RAP in flow buffer (15 μM) was measured at the flow rate of 10 μL/min at 20 °C. [b] Interactions were significantly reduced upon addition of DTT. [c] Interaction is not detected (nd).

Table 2: SPR Analysis of GST/RAP Repeat Constructs Binding to ERp57[a]

	k_a (1/Ms)	k_d (1/s)	K_A (1/M)	K_D (M)
GST	nd[b]	nd[b]	nd[b]	nd[b]
GST/RAP (1−323)	1.03×10^6	1.47×10^{-3}	7.01×10^8	1.43×10^{-9}
GST/RAP (1−110)	8.16×10^5	1.44×10^{-3}	5.66×10^8	1.77×10^{-9}
GST/RAP (91−210)	3.82×10^5	1.78×10^{-3}	2.15×10^8	4.66×10^{-9}
GST/RAP (221−323)	2.45×10^5	1.56×10^{-3}	1.57×10^8	6.37×10^{-9}

[a] ERp57 was immobilized on a sensor chip, and the binding of GST/RAP constructs in flow buffer (15 μM) was measured at the flow rate of 10 μL/min at 20 °C. [b] Interaction is not detected (nd).

tion. RAP contains an internal triplicate repeat structure with three equally divided regions sharing high homology (*15*, *34*). Our previous studies have shown that the high-affinity LRP binding sites within RAP localize to its carboxyl-terminal repeat (repeat 3) (*13*, *35*). To assess whether RAP utilizes similar or different epitopes to bind ERp57, we examined the interactions between our GST/RAP repeat constructs and ERp57 via SPR. As seen in Table 2, GST/RAP constructs consisting of either full-length (1−323) or repeat 1 of RAP (1−110) bind to ERp57 with similarly high affinity, suggesting the existence of a high-affinity binding

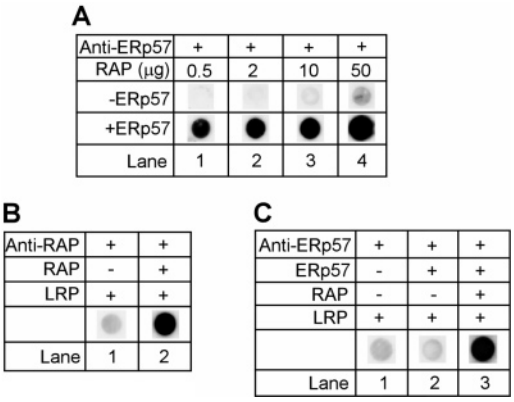

FIGURE 9: RAP is capable of bridging an interaction between ERp57 and LRP. (A) Buffer alone (−ERp57) or buffer containing recombinant ERp57 (1 μg, +ERp57) was blotted on a PVDF membrane, followed with binding of RAP at increasing concentrations as indicated. Bound RAP was detected with anti-RAP antibody. (B) Purified human placental LRP (0.5 μg) was blotted on the PVDF membrane, followed with binding of buffer alone or buffer containing RAP (1 nM). The bound RAP was detected with anti-RAP antibody. (C) Purified LRP on the PVDF membrane as in B was incubated with buffer alone or buffer containing RAP (1 nM). After washing and blocking, we incubated the membrane further with buffer alone or buffer containing ERp57 (1 nM). Bound ERp57 was detected with an anti-ERp57 antibody. Note the fact that ERp57 binds to LRP only with a prior incubation of RAP demonstrates an ability for RAP to bridge ERp57−LRP interaction.

site within the first repeat of RAP. GST/RAP constructs consisting of either repeat 2 (91−210) or repeat 3 (221−323) bind to ERp57 with reduced affinity compared to full-length RAP. Taken together, these results suggest that there are likely at least three distinct ERp57-binding epitopes within RAP that are distributed throughout the entire RAP sequence, with the amino-terminal repeat site possessing the highest affinity. The higher affinity of GST/RAP to ERp57 when compared to RAP (without GST) may reflect the difference in the assembly states of GST/RAP and RAP because GST itself does not bind to ERp57 (Table 2).

To further confirm binding of RAP to ERp57 using alternative methods, we performed a ligand dot-blot assay. As seen in Figure 9A, ERp57 is able to bind RAP in a dose-dependent manner, consistent with our results obtained by SPR analysis.

RAP Is Capable of Binding LRP and ERp57 Simultaneously. One possible role of the RAP−ERp57 interaction is to recruit this oxidoreductase to LRP during receptor folding. Therefore, we examined whether RAP is capable of mediating an interaction between ERp57 and LRP. As a positive control, LRP purified from human placenta was blotted onto a PVDF membrane, followed by binding of RAP and detection with anti-RAP antibody (Figure 9B). As expected, RAP binds to purified LRP with high affinity. The ability of ERp57 to bind to either LRP alone or to LRP that has been previously incubated with RAP was assessed by blotting with an antibody to ERp57 (Figure 9C). We found that, although ERp57 alone does not bind to LRP (Figure 9C, lane 2), it is capable of binding to RAP that has been previously bound to LRP (Figure 9C, lane 3). These results demonstrate that RAP can mediate an interaction between LRP and ERp57.

DISCUSSION

The complex structures of the LDL receptor family members, due largely to the extensive intradomain disulfide bonds, present a challenging task for proper folding. At the same time, they provide an unique opportunity to study protein folding that involves the choreographic actions of protein modification and of molecular chaperones. For example, each LRP molecule contains 159 disulfide bonds within its ligand-binding and EGF repeats; therefore, protection of free cysteines prior to disulfide linkage and proper positioning of paired cysteines during disulfide formation may account for the majority of the LRP folding process. A cooperative interaction of general ER chaperones (e.g., BiP, PDI, and calnexin) and specialized chaperones (e.g., RAP) within the ER is likely involved in this process. Our current studies demonstrate that protein posttranslational modifications such as N-linked glycosylation also play pivotal roles in LRP folding. We further show that, although RAP functions independently from N-linked glycosylation during LRP folding and disulfide linkage, it interacts with general ER chaperones even when they are bound to LRP. These studies provide significant insight into how various factors coordinate with one another during the complex folding process of LRP.

LRP glycosylation was initially described by biochemical studies indicating that carbohydrates, largely N-linked, contribute to ~18% of the size of the 515 kDa ligand-binding subunit and to ~25% of the 85 kDa transmembrane subunit (*29*). It was suggested that these carbohydrates modifications of LRP may contribute to ligand binding as the lectin WGA, which binds saccharides on LRP, partially inhibiting α2-macroglobulin and RAP binding. However, our current results clearly show that RAP is capable of binding nonglycosylated LRP during receptor folding. More recently, studies by May et al. (*36*) have shown that LRP is differentially glycosylated in different tissues. The authors further demonstrated that hypoglycosylation of LRP correlates with an increased shedding of the LRP ectodomain, which results in an increased substrate availability for γ-secretase cleavage and the release of the LRP intracellular domain (*36*, *37*). Given our current results demonstrating a role for N-linked glycosylation in LRP folding, it is tempting to speculate that the differences in LRP glycosylation state may dictate its folding/conformation such that the accessibility to membrane-anchoring proteases (e.g., members of the metalloprotease family) is variable. Our LRP minireceptors bearing mutations at individual N-linked glycosylation sites should allow this to be tested directly.

Recently, the molecular mechanism underlying the role of N-linked glycosylation in protein folding has become increasingly clear. In addition to providing bulky modification for spatial constraint, the highly hydrophilic groups also help to maintain glycoproteins in solution during folding (*23*). More importantly, convincing studies have shown that ER lectins calnexin/calreticulum retain not yet properly folded molecules in the ER by interacting with N-linked monoglucosylated oligosaccharides (*23*, *30*). The glucosylation of folding intermediates is carried out by UDP-glucose glycoprotein glucosyltransferase, which is believed to possess the ability to sense the folding states of glycoproteins (*23*, *30*). Although our current results, as well as those by Orlando et al. (*38*), clearly demonstrate an interaction between LRP and calnexin, LRP minireceptors bearing different glycosylation mutations exhibit variable binding to calnexin such that binding did not correlate with the degree of receptor misfolding. These results suggest that the cycle of glucosylation and deglucosylation does not necessarily provide the only sensor for misfolded glycoproteins, and other ER chaperones such as BiP and several disulfide isomerases (e.g., PDI and ERp57) may participate in this quality control process. Nevertheless, the roles of N-linked glycosylation of LRP likely include binding of calnexin/calreticulin during folding.

A recent study has systematically dissected a cotranslational folding pathway of influenza hemagglutinin (HA) (*39*). It was shown that multiple glycans that are positioned at critical regions are essential for binding by the chaperones, calnexin and calreticulin, and the oxidoreductase, ERp57. It is interesting to note that the positioning of glycans seems to be strategically placed near cysteine residues such that improper and premature disulfide bond formation can be minimized. Intriguingly, when the positions of *N*-glycans within the four clusters of LRP ligand-binding and EGF repeats were examined, 11 out of 22 sites are found next to cysteine residues. The average distance of all 22 *N*-glycans to cysteine is 1.1 residues, whereas the calculated random distance would be 3.4 residues. Thus the placement of *N*-glycans near cysteine residues further suggests a role of N-linked glycosylation in the protection of cysteine residues prior to disulfide bond linkage and/or recruitment of calnexin/calreticulin-bound ERp57 to the proper sites for correct disulfide bond formation. Future mutagenesis analysis directed at individual glycosylation sites should generate further insight into the functions of *N*-glycan during LRP folding.

Our previous studies have clearly demonstrated a role of RAP in the proper folding and disulfide formation of LRP (*11*, *12*, *14*, *16*). In the absence of RAP coexpression, LRP minireceptors are oligomerized due to formation of mislinked intermolecular disulfide bonds, suggesting that interactions between RAP and multiple sites on LRP are important for ensuring proper linkage of intradomain but not interdomain or intermolecular disulfide bonds. However, since RAP itself does not contain any cysteine residues, how it achieves this unique function was not clear. One possibility is that it functions similarly to those of N-linked glycosylation by providing proper spatial constraints during receptor folding.

Recent evidence has shown that ER chaperones interact with one another in a coordinated fashion and exist in large complexes during protein folding. For example, ERp57 is found in MHC class I heavy chain complexes with calnexin that are generated early during the MHC class I assembly pathway (*40*). The oxidoreductase activity of ERp57 suggests that it is involved in disulfide bond formation (*40*, *41*). Further NMR studies revealed interaction between ERp57 and the tip of the calreticulin P-domain (*42*). Given the high content of disulfide bonds in LRP, it is likely that calnexin/calreticulin bound to LRP through N-linked glycosylation plays an important role in recruiting oxidoreductases (e.g., ERp57) into the local environment where disulfide bond formation/rearrangement takes place (*31*, *32*). Our current studies also demonstrate an interaction between RAP and ERp57 by both SPR and dot-blot analyses, suggesting that at least one of the roles of RAP in LRP folding is to recruit

oxidoreductases to the proper site and/or increase local availability of these enzymes. We have attempted to perform co-immunoprecipitation experiments between endogenous RAP and ERp57. However, multiple attempts failed. This may be due to either a very transient interaction in vivo and/or a low affinity between these chaperones to survive co-immunoprecipitation. Interestingly, the ERp57-binding sites appear to localize within the amino-terminus of RAP, whereas those for LRP binding reside within its carboxyl-terminus. These results are consistent with our findings that RAP is capable of bridging the interaction between oxidoreductase and LRP. Together, these results suggest independent, yet similar, roles for N-linked glycosylation-bound calnexin/calreticulin and RAP in recruiting oxidoreductases to LRP during folding. Whether the function of Mesd/Boca as a specialized chaperone for LDL receptor family members is also involved in the recruitment of general ER chaperones remains to be investigated.

In summary, the roles of various factors and molecular chaperones in the complex folding process of LRP are now beginning to emerge. First, Ca^{2+} ions likely function as a nucleation site during initial folding of ligand-binding repeats (*11*). Second, N-linked glycosylation and RAP/Mesd bound at various sites along the receptor may provide appropriate spatial constraints and local environments that are optimal for receptor folding. Third, retention of folding intermediates is likely achieved by a combination of lectin chaperone binding to monoglucosylated sites and BiP/oxidoreductases. Finally, the extensive disulfide bond formation is achieved by a cooperative action between the specialized chaperone RAP and general ER chaperones such as ERp57. Such a complex folding process determines that any disruption in these events will lead to receptor misfolding. The detailed molecular mechanisms await reconstitution studies using semi in vivo or in vitro approaches.

REFERENCES

1. Herz, J., and Strickland, D. K. (2001) LRP: a multifunctional scavenger and signaling receptor, *J. Clin. Invest. 108*, 779−784.
2. Herz, J., and Bock, H. H. (2002) Lipoprotein receptors in the nervous system, *Annu. Rev. Biochem. 71*, 405−434.
3. Herz, J., Kowal, R. C., Goldstein, J. L., and Brown, M. S. (1990) Proteolytic processing of the 600 kd low density lipoprotein receptor-related protein (LRP) occurs in a trans-Golgi compartment, *EMBO J. 9*, 1769−1776.
4. Willnow, T. E., Moehring, J. M., Inocencio, N. M., Moehring, T. J., and Herz, J. (1996) The low-density-lipoprotein receptor-related protein (LRP) is processed by furin in vivo and in vitro, *Biochem. J. 313*, 71−76.
5. Jeon, H., Meng, W., Takagi, J., Eck, M. J., Springer, T. A., and Blacklow, S. C. (2001) Implications for familial hypercholesterolemia from the structure of the LDL receptor YWTD-EGF domain pair, *Nat. Struct. Biol. 8*, 499−504.
6. Daly, N. L., Djordjevic, J. T., Kroon, P. A., and Smith, R. (1995) Three-dimensional structure of the second cysteine-rich repeat from the human low-density lipoprotein receptor, *Biochemistry 34*, 14474−14481.
7. Daly, N. L., Scanlon, M. J., Djordjevic, J. T., Kroon, P. A., and Smith, R. (1995) Three-dimensional structure of a cysteine-rich repeat from the low-density lipoprotein receptor, *Proc. Natl. Acad. Sci. U.S.A. 92*, 6334−6338.
8. Fass, D., Blacklow, S., Kim, P. S., and Berger, J. M. (1997) Molecular basis of familial hypercholesterolaemia from structure of LDL receptor module, *Nature 388*, 691−693.
9. Huang, W., Dolmer, K., and Gettins, P. G. (1999) NMR solution structure of complement-like repeat CR8 from the low density lipoprotein receptor-related protein, *J. Biol. Chem. 274*, 14130−14136.
10. Koduri, V., and Blacklow, S. C. (2001) Folding determinants of LDL receptor type A modules, *Biochemistry 40*, 12801−12807.
11. Obermoeller, L. M., Chen, Z., Schwartz, A. L., and Bu, G. (1998) Ca^{2+} and receptor-associated protein are independently required for proper folding and disulfide bond formation of the low density lipoprotein receptor-related protein, *J. Biol. Chem. 273*, 22374−22381.
12. Bu, G., and Rennke, S. (1996) Receptor-associated protein is a folding chaperone for low density lipoprotein receptor-related protein, *J. Biol. Chem. 271*, 22218−22224.
13. Obermoeller, L. M., Warshawsky, I., Wardell, M. R., and Bu, G. (1997) Differential functions of triplicated repeats suggest two independent roles for the receptor-associated protein as a molecular chaperone, *J. Biol. Chem. 272*, 10761−10768.
14. Obermoeller-McCormick, L., Li, Y., Osaka, H., FitzGerald, D., Schwartz, A., and Bu, G. (2001) Dissection of receptor folding and ligand-binding property with functional minireceptors of LDL receptor-related protein, *J. Cell Sci. 114*, 899−908.
15. Bu, G., Geuze, H. J., Strous, G. J., and Schwartz, A. L. (1995) 39 kDa receptor-associated protein is an ER resident protein and molecular chaperone for LDL receptor-related protein, *EMBO J. 14*, 2269−2280.
16. Bu, G., and Schwartz, A. L. (1998) RAP, a novel type of ER chaperone, *Trends Cell Biol. 8*, 272−276.
17. Bu, G. (2001) The roles of receptor-associated protein (RAP) as a molecular chaperone for members of the LDL receptor family, *Int. Rev. Cytol. 209*, 79−116.
18. Hsieh, J. C., Lee, L., Zhang, L., Wefer, S., Brown, K., DeRossi, C., Wines, M. E., Rosenquist, T., and Holdener, B. C. (2003) Mesd encodes an LRP5/6 chaperone essential for specification of mouse embryonic polarity, *Cell 112*, 355−367.
19. Culi, J., and Mann, R. S. (2003) Boca, an endoplasmic reticulum protein required for wingless signaling and trafficking of LDL receptor family members in Drosophila, *Cell 112*, 343−354.
20. He, X., Semenov, M., Tamai, K., and Zeng, X. (2004) LDL receptor-related proteins 5 and 6 in Wnt/beta-catenin signaling: arrows point the way, *Development 131*, 1663−1677.
21. Hammond, C., Braakman, I., and Helenius, A. (1994) Role of N-linked oligosaccharide recognition, glucose trimming, and calnexin in glycoprotein folding and quality control, *Proc. Natl. Acad. Sci. U.S.A. 91*, 913−917.
22. Hammond, C., and Helenius, A. (1994) Folding of VSV G protein: sequential interaction with BiP and calnexin, *Science 266*, 456−458.
23. Parodi, A. J. (2000) Protein glucosylation and its role in protein folding, *Annu. Rev. Biochem. 69*, 69−93.
24. Ellgaard, L., and Helenius, A. (2001) ER quality control: towards an understanding at the molecular level, *Curr. Opin. Cell Biol. 13*, 431−437.
25. Willnow, T. E., Rohlmann, A., Horton, J., Otani, H., Braun, J. R., Hammer, R. E., and Herz, J. (1996) RAP, a specialized chaperone, prevents ligand-induced ER retention and degradation of LDL receptor-related endocytic receptors, *EMBO J. 15*, 2632−2639.
26. Bu, G., Maksymovitch, E. A., Geuze, H., and Schwartz, A. L. (1994) Subcellular localization and endocytic function of low density lipoprotein receptor-related protein in human glioblastoma cells, *J. Biol. Chem. 269*, 29874−29882.
27. Bu, G., Maksymovitch, E. A., and Schwartz, A. L. (1993) Receptor-mediated endocytosis of tissue-type plasminogen activator by low density lipoprotein receptor-related protein on human hepatoma HepG2 cells, *J. Biol. Chem. 268*, 13002−13009.
28. Laemmli, U. K. (1970) Cleavage of structural proteins during the assembly of the head of bacteriophage T4, *Nature 227*, 680−685.
29. Jensen, P. H., Gliemann, J., and Orntoft, T. (1992) Characterization of carbohydrates in the alpha 2-macroglobulin receptor, *FEBS Lett. 305*, 129−132.
30. Ellgaard, L., and Helenius, A. (2003) Quality control in the endoplasmic reticulum, *Nat. Rev. Mol. Cell Biol. 4*, 181−191.
31. Oliver, J. D., van der Wal, F. J., Bulleid, N. J., and High, S. (1997) Interaction of the thiol-dependent reductase ERp57 with nascent glycoproteins, *Science 275*, 86−88.
32. Oliver, J. D., Roderick, H. L., Llewellyn, D. H., and High, S. (1999) ERp57 functions as a subunit of specific complexes formed with the ER lectins calreticulin and calnexin, *Mol. Biol. Cell 10*, 2573−2582.

33. Urade, R., Okudo, H., Kato, H., Moriyama, T., and Arakaki, Y. (2004) ER-60 domains responsible for interaction with calnexin and calreticulin, *Biochemistry 43*, 8858−8868.
34. Ellgaard, L., Holtet, T. L., Nielsen, P. R., Etzerodt, M., Gliemann, J., and Thogersen, H. C. (1997) Dissection of the domain architecture of the alpha2macroglobulin-receptor-associated protein, *Eur. J. Biochem. 244*, 544−551.
35. Melman, L., Cao, Z., Rennke, S., Marzolo, M. P., Wardell, M. R., and Bu, G. (2001) High affinity binding of receptor-associated protein to heparin and low density lipoprotein receptor-related protein requires similar basic amino acid sequence motifs, *J. Biol. Chem. 276*, 29338−29346.
36. May, P., Bock, H. H., Nimpf, J., and Herz, J. (2003) Differential glycosylation regulates processing of lipoprotein receptors by gamma-secretase, *J. Biol. Chem. 278*, 37386−37392.
37. May, P., Reddy, Y. K., and Herz, J. (2002) Proteolytic processing of low density lipoprotein receptor-related protein mediates regulated release of its intracellular domain, *J. Biol. Chem. 277*, 18736−18743.
38. Orlando, R. A. (2004) The low-density lipoprotein receptor-related protein associates with calnexin, calreticulin, and protein disulfide isomerase in receptor-associated-protein-deficient fibroblasts, *Exp. Cell Res. 294*, 244−253.
39. Daniels, R., Kurowski, B., Johnson, A. E., and Hebert, D. N. (2003) N-linked glycans direct the cotranslational folding pathway of influenza hemagglutinin, *Mol. Cell 11*, 79−90.
40. Lindquist, J. A., Jensen, O. N., Mann, M., and Hammerling, G. J. (1998) ER-60, a chaperone with thiol-dependent reductase activity involved in MHC class I assembly, *EMBO J. 17*, 2186−2195.
41. Urade, R., Kusunose, M., Moriyama, T., Higasa, T., and Kito, M. (2000) Accumulation and degradation in the endoplasmic reticulum of a truncated ER-60 devoid of C-terminal amino acid residues, *J. Biochem. 127*, 211−220.
42. Frickel, E. M., Riek, R., Jelesarov, I., Helenius, A., Wuthrich, K., and Ellgaard, L. (2002) TROSY-NMR reveals interaction between ERp57 and the tip of the calreticulin P-domain, *Proc. Natl. Acad. Sci. U.S.A. 99*, 1954−1959.

BI047652A